AXIS INTERNATIONAL JOURNAL OF MULTIDISCIPLINARY RESEARCH (AIJMR)
Peer review journal As per UGC 2025 Standard Guidelines

DEVELOPMENT AND PERFORMANCE ASSESSMENT OF ADVANCED THERMOELECTRIC MATERIALS FOR SUSTAINABLE ENERGY CONVERSION IN CHHATTISGARH

[1]Megha Dewangan,[2]Dr. Alok Bhatt (Professor)

[1]Research Scholar, [2]Supervisor
[1-2]Department of Physics, Bharti Vishwavidyalaya, Durg, Chhattisgarh

ABSTRACT

Thermoelectric materials convert a temperature difference directly into electrical power and are therefore attractive for distributed waste-heat recovery where reliability, compactness and the absence of moving parts are important. This analytical paper assesses three advanced material families—Bi_2Te_3-based alloys, SnSe-based materials and doped oxide thermoelectrics—for sustainable energy-conversion opportunities relevant to Chhattisgarh. The study uses a descriptive-analytical design based on peer-reviewed experimental literature and official regional information; it does not claim new laboratory measurements. Performance is interpreted through the Seebeck coefficient, electrical conductivity, thermal conductivity, power factor and dimensionless figure of merit ZT, together with a constant-property upper-bound efficiency model. Published results show the complementary nature of the three families: Bi_2Te_3 remains strong near ambient and low-grade heat, SnSe provides exceptionally high peak and average ZT across low-to-medium temperature ranges when carrier and crystal structures are engineered, while oxide systems such as $Ca_3Co_4O_9$ offer chemical and thermal robustness at higher temperatures despite lower ZT. Representative Chhattisgarh screening cases yield idealized efficiencies of approximately 5.5% for Bi_2Te_3 at 423/313 K, 13.3% for SnSe at 673/313 K and 5.0% for a doped oxide case at 873/323 K. These values are upper-bound comparisons rather than device predictions. The analysis concludes that material selection should be temperature-window-specific: Bi_2Te_3 for low-grade surfaces and flexible devices, SnSe for higher-performance medium-grade recovery, and oxides for harsher high-temperature environments. A staged research pathway is proposed for local validation, including thermal mapping, material processing, contact engineering, module testing and long-duration stability assessment.

Keywords: thermoelectric materials; Bi_2Te_3; SnSe; oxide thermoelectrics; $Ca_3Co_4O_9$; figure of merit; waste-heat recovery; sustainable energy; Chhattisgarh.

ARTICLE HISTORY

Received: 27 April 2026, Accepted: 20 May 2026, Published: 25 June 2026

CITATION

Dewangan. M., Bhatt, A., (2026). Development and Performance Assessment of Advanced Thermoelectric Materials for Sustainable Energy Conversion in Chhattisgarh. *AXIS International Journal of Multidisciplinary Research (AIJMR),* 2(1), 1-11.
DOI:

Introduction

Energy conversion in an industrial economy is accompanied by heat rejection at many temperatures. Conventional recovery systems are most attractive when heat sources are large and thermodynamically concentrated, whereas many real surfaces, ducts, pipes, enclosures and intermittent processes release heat in distributed form. Thermoelectric generators (TEGs) address

this niche by exploiting coupled electrical and thermal transport in solids. A temperature gradient produces a Seebeck voltage, and a closed electrical circuit permits useful power to be delivered without a rotating machine or working fluid. The same device can operate in reverse for Peltier cooling, but the present study concentrates on electricity generation from waste heat. The central materials challenge is that a good thermoelectric must simultaneously sustain a large Seebeck coefficient, high electrical conductivity and low thermal conductivity. These transport requirements are strongly coupled. Increasing carrier concentration usually improves electrical conductivity but can reduce the Seebeck coefficient and increase electronic heat conduction. Modern thermoelectric development therefore relies on band engineering, defect chemistry, alloying, nanostructuring, texturing, phonon scattering, carrier optimization and contact design rather than on a single-property improvement.

For Chhattisgarh, a material assessment is particularly relevant because the state presents a combination of energy-intensive industry and a warm seasonal environment. The Government of Chhattisgarh identifies major steel-sector growth drivers including iron ore, coal and limestone reserves, established anchor units and more than 26,000 MW of installed power capacity. This industrial profile does not by itself quantify recoverable waste heat, but it provides a rational basis for evaluating thermoelectric technologies that can be attached to hot industrial surfaces and auxiliary systems. The climatic cold-side constraint is also important: the India Meteorological Department 1991–2020 normal for Raipur records a mean daily maximum of 41.8 °C in May, which can reduce available temperature difference unless heat sinking is carefully designed.

1.1 Research Problem

High laboratory ZT does not automatically translate into useful field energy conversion. A material may have excellent intrinsic transport properties but perform poorly in a generator because of anisotropy, contact resistance, thermal expansion mismatch, oxidation, mechanical weakness, expensive processing or an operating temperature that does not match the available heat source. Conversely, an intrinsically lower-ZT material can be valuable if it survives temperatures and atmospheres that rapidly degrade a higher-ZT competitor. The research problem is therefore not simply to identify the largest reported ZT; it is to determine which thermoelectric material family offers the most appropriate combination of performance, temperature compatibility, stability and manufacturability for realistic Chhattisgarh energy-conversion conditions.

1.2 Objectives of the Study

- To explain the physics governing Seebeck conversion, power factor, thermal transport and thermoelectric figure of merit.
- To examine the development strategies and reported performance of Bi_2Te_3-based, SnSe-based and doped oxide thermoelectric materials.
- To compare low-, medium- and high-temperature material options using a common analytical efficiency framework.
- To interpret how Chhattisgarh industrial context and warm ambient conditions influence thermal matching and cold-side design.
- To evaluate stability, manufacturability, contact engineering and sustainability constraints in addition to peak ZT.

2. Review of Literature

Bi_2Te_3 and its alloys form the benchmark class for near-room-temperature thermoelectrics. Venkatasubramanian et al. (2001) demonstrated very high room-temperature thermoelectric performance in Bi_2Te_3/Sb_2Te_3 superlattice thin films, establishing the power of low-dimensional transport engineering. Poudel et al. (2008) later showed that bulk nanostructured p-type bismuth–antimony telluride could reach a peak ZT of about 1.4 near 373 K while retaining bulk form, illustrating how boundary scattering can suppress lattice heat transport without destroying electrical conduction. More recently, Zheng et al. (2023) demonstrated flexible Ag-doped Bi_2Te_3 films with room-temperature ZT around 1.2 and a 40-pair device power density of 2.1 mW cm^{-2} at a temperature difference of 64 K. Together these studies show that Bi_2Te_3 is not a static “old” thermoelectric but a platform continually improved through nanostructure, texture and device architecture.

SnSe shifted the high-performance thermoelectric landscape after Zhao et al. (2014) reported p-type single-crystal SnSe with exceptionally low lattice thermal conductivity and peak ZT of 2.6 ± 0.3 at 923 K along the b axis. Duong et al. (2016) established high-performance n-type SnSe through Bi doping, reporting peak ZT around 2.2 at 733 K. A major practical objection to early SnSe work was the difficulty of reproducing single-crystal performance in scalable polycrystals. Zhou et al. (2021) addressed this by purification and Na doping, reporting polycrystalline SnSe with peak ZT about 3.1 at 783 K. Qin et al. (2023) then demonstrated that structural modulation of p-type SnSe could produce an average ZT near 2.0 from 300–673

K and single-leg conversion efficiency about 8.9% across a temperature difference near 300 K. These results move SnSe from a high-ZT material example toward device-relevant medium-temperature conversion.

Oxide thermoelectrics occupy a different design space. Their ZT values are generally lower than leading chalcogenides, but ionic/covalent bonding and chemical stability can make them attractive at elevated temperature and in oxidizing atmospheres. Hira et al. (2022) showed that Na/Mo dual doping of $Ca_3Co_4O_9$ increased power factor and reduced resistive/thermal losses, producing ZT about 0.27 at 1000 K—roughly 2.5 times their parent composition. Merkulov et al. (2021) demonstrated a 12-couple tubular module using p-type $Ca_3Co_4O_9$ and n-type $Ca_{0.95}Pr_{0.05}MnO_3$ grown by laser floating zone processing, with power output up to 20 mW at a 389 °C temperature gradient and 525 °C hot side. These values are smaller than chalcogenide efficiencies, but they illustrate the importance of stability, geometry and contacts when the operating temperature is high

Table 1. Thematic synthesis of literature used in the analytical assessment.

Theme	Representative studies	Main contribution	Relevance to this paper
Near-room-temperature chalcogenides	Venkatasubramanian et al. (2001); Poudel et al. (2008); Zheng et al. (2023)	Superlattice, nanostructured bulk and flexible-film Bi_2Te_3 strategies	Defines the low-grade heat benchmark and mature material family
High-performance SnSe	Zhao et al. (2014); Duong et al. (2016); Zhou et al. (2021)	High p- and n-type ZT; suppression of lattice thermal conductivity; scalable polycrystal route	Defines the medium-temperature high-performance candidate
Device-relevant SnSe	Qin et al. (2023); Shi et al. (2025)	High average ZT and measured single-leg efficiencies	Shows why average ZT and contacts matter more than peak ZT alone
High-temperature oxides	Saini et al. (2017); Hira et al. (2022); Merkulov et al. (2021)	Doping, defect engineering and oxide module demonstration	Provides a stability-oriented option for harsher thermal environments
Regional thermal context	Govt. of Chhattisgarh; India Meteorological Department	Industrial concentration and Raipur climate normals	Supports local operating-window and cold-side interpretation

3. Research Methodology

The study adopts a descriptive-analytical research design. It is descriptive because it organizes established thermoelectric physics, material-development strategies and experimental performance reported in the literature. It is analytical because the same physical metrics and efficiency equation are used to compare material families under representative Chhattisgarh temperature scenarios. The scientific evidence base consists primarily of peer-reviewed experimental papers published between 2001 and 2026. Official Government of Chhattisgarh and India Meteorological Department sources are used only for regional industrial and climatic context. No field survey, proprietary plant data or new laboratory measurement is presented.

Three material families are selected because they represent distinct thermal regimes and engineering trade-offs: (i) Bi_2Te_3-based alloys for near-ambient and low-grade heat, (ii) SnSe-based materials for high-performance low-to-medium and medium-temperature conversion, and (iii) doped oxide thermoelectrics, represented mainly by $Ca_3Co_4O_9$-based p-type systems, for higher-temperature oxidizing service. The analytical unit is a thermoelectric leg or effective p–n couple characterized by Seebeck coefficient S, electrical conductivity σ, thermal conductivity κ, temperature T and dimensionless figure of merit ZT.

Performance assessment has two levels. First, reported literature data are compared without treating unlike geometries as directly equivalent. Peak ZT, average ZT, temperature range and device demonstrations are interpreted as complementary evidence rather than merged into a single ranking. Second, a constant-property maximum-efficiency expression is evaluated using representative hot-side temperature T_h, cold-side temperature Tc and effective average ZT. The calculation is deliberately an upper-bound screening model: it assumes material properties can be represented by a temperature-averaged ZT and excludes parasitic heat loss, electrical/thermal contact resistance, radiation, convective bypass, electrode losses and geometry-specific current crowding. Therefore, calculated efficiencies are not predictions of field-module efficiency.

Table 2. Methodological framework.

Element	Description	Purpose
Design	Descriptive-analytical literature assessment	Explain physics and compare materials using a common framework
Scientific sources	Peer-reviewed experimental thermoelectric studies, 2001–2026	Ground material claims in measured literature
Regional sources	Chhattisgarh industry portal and IMD climatological normal	Define local context without inventing plant measurements
Variables	S, σ, κ, PF, ZT, T_h, Tc, η	Link materials physics to conversion performance
Model	Constant-property ideal thermoelectric efficiency	Provide comparable upper-bound screening values
Scope limitation	No field heat-flux map, lifecycle inventory or prototype test	Keep conclusions analytical rather than empirical

4. Physics of Thermoelectric Energy Conversion

The Seebeck effect is the starting point for thermoelectric generation. When a homogeneous conducting material experiences a temperature difference, charge carriers diffuse from the hot region toward the cold region and establish an electrochemical potential. For a small temperature interval, the open-circuit voltage is approximately proportional to the temperature difference. In a practical p–n couple the useful voltage is the difference between the p-type and n-type Seebeck responses, so material pairing is as important as the absolute Seebeck coefficient of either leg.

$$V_o c = (S_p - S_n)\,\Delta T$$

Open-circuit voltage of an ideal p–n thermoelectric couple.

$$PF = S^2\sigma = S^2/\rho$$

Power factor; ρ is electrical resistivity and σ = 1/ρ.

$$ZT = S^2\sigma T / \kappa = S^2 T /(\rho\kappa)$$

Dimensionless thermoelectric figure of merit; $\kappa = \kappa_e + \kappa_l$.

The figure of merit expresses a competition between electronic usefulness and thermal leakage. A large S and σ increase electrical output, while a small κ maintains the temperature gradient. The total thermal conductivity contains electronic and lattice contributions. Heavy doping can raise σ but also increases κ_e, approximately following the Wiedemann–Franz relation $\kappa_e = L\sigma T$ when a suitable Lorenz number L is used. Nanostructuring and alloy disorder seek to reduce κ_l by scattering phonons more strongly than charge carriers. Band convergence and resonant or defect levels seek to improve electronic transport without proportionally increasing heat leakage. The central development problem is therefore transport decoupling.

$$\eta_{max} = ((T_h - Tc)/T_h) \cdot [\,(\sqrt{(1+Z\bar{T})} - 1) / (\sqrt{(1+Z\bar{T})} + Tc/T_h)\,]$$

Constant-property maximum-efficiency expression used for analytical screening.

The first factor is Carnot efficiency; the second describes thermoelectric irreversibility for an effective average $Z\bar{T}$. Raising hot-side temperature increases the thermodynamic driving force but may also change phase stability, carrier concentration, contact reaction and radiation loss. Similarly, improving ZT at a single temperature is less valuable than maintaining high ZT over the full leg temperature profile. This distinction explains why recent SnSe studies increasingly report average ZT and measured single-leg efficiency rather than only the highest point on a ZT–T curve.

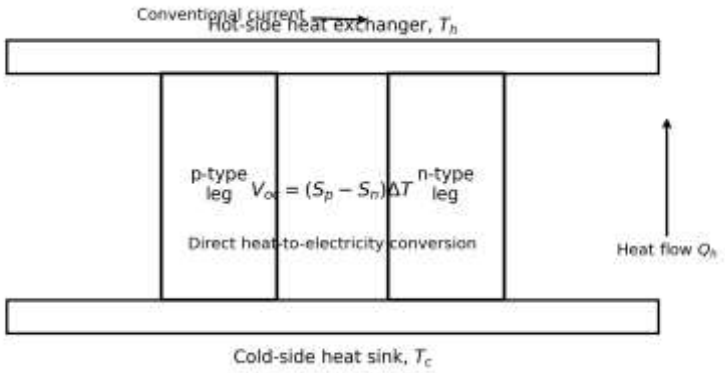

Figure 1. Physics schematic of a thermoelectric p–n couple under a temperature gradient.

Table 3. Key physical metrics and their design significance.

Metric	Expression / unit	Physical interpretation	Design implication
Seebeck coefficient, S	V K^{-1}	Voltage generated per temperature difference	Large |S| increases voltage
Electrical conductivity, σ	S m^{-1}	Carrier transport capability	High σ reduces Joule loss
Thermal conductivity, κ	W m^{-1} K^{-1}	Heat leakage through the leg	Low κ preserves ΔT
Power factor, PF	$S^2\sigma$	Electrical transport quality	Useful for power-density screening
Figure of merit, ZT	$S^2\sigma T/\kappa$	Coupled thermoelectric quality	Higher ZT improves ideal efficiency
Average ZT, $Z\bar{T}$	Temperature-averaged	Performance across the whole leg	More relevant to device efficiency than peak alone

5. Development and Performance of SnSe-Based Thermoelectrics

Tin selenide is a layered orthorhombic semiconductor whose low-symmetry bonding produces strongly anisotropic electrical and thermal transport. Its thermoelectric importance arises from an unusual combination of favorable electronic structure and extremely low lattice thermal conductivity. Zhao et al. (2014) reported a peak p-type ZT of 2.6 ± 0.3 at 923 K along the b axis of single crystals, with lattice thermal conductivity falling to roughly 0.23 W m^{-1} K^{-1} near 973 K. The result established SnSe as a leading high-ZT material, but it also highlighted challenges of anisotropy, single-crystal growth and reproducibility. Development proceeded in two directions: obtaining high-performance n-type SnSe and transferring single-crystal physics into scalable polycrystalline forms. Duong et al. (2016) used Bi doping to realize n-type SnSe with peak ZT around 2.2 at 733 K along the b direction. Zhou et al. (2021) showed that purification is crucial because oxidation-related or impurity phases can increase thermal conductivity. Their purified, Na-doped polycrystalline SnSe reached peak ZT around 3.1 at 783 K, demonstrating that a polycrystalline route can exceed earlier single-crystal peak values when carrier density and impurity control are optimized.

6. Doped Oxide Thermoelectrics for High-Temperature Conversion

Oxide thermoelectrics are selected for this study because they address the high-temperature stability problem from a different direction. Calcium cobaltite $Ca_3Co_4O_9$ is a layered misfit oxide that provides p-type conduction and relatively high Seebeck coefficient at elevated temperature. Its total ZT is lower than the best Bi_2Te_3 or SnSe systems, but it uses thermally robust oxide chemistry and can operate in air at temperatures where many telluride or selenide compositions require stronger encapsulation. Complementary n-type oxide legs include doped $CaMnO_3$, ZnO-based compounds and In_2O_3-based systems. Doping is used to tune both carrier transport and phonon scattering. Saini et al. (2017) studied Tb substitution in $Ca_3Co_4O_9$ as a route to higher thermoelectric performance. Hira et al. (2022) used simultaneous Na and Mo substitution in $Ca_3Co_4O_9$. Their optimum $Ca_{2.95}Na_{0.05}Co_{3.975}Mo_{0.025}O_9$ composition showed a maximum power factor near 3.2 × 10^{-4} W m^{-1} K^{-2} and ZT about 0.27 at 1000 K, about 2.5 times the undoped parent in that study. The improvement arose from a combined enhancement of Seebeck response with reductions in resistivity and thermal conductivity.

Table 5. High-temperature oxide thermoelectric trade-offs.

Attribute	$Ca_3Co_4O_9$-based response	Advantage	Constraint
Thermal stability	Designed for elevated-temperature oxide service	Better compatibility with hot oxidizing environments	Contacts and n-type partner still limit module
Transport development	Doping adjusts carrier density, Seebeck response and phonon scattering	Multiple defect-chemistry routes	ZT remains below leading chalcogenides
Representative result	Na/Mo dual-doped ZT ≈ 0.27 at 1000 K	Large gain over parent composition in the same study	Peak value still modest for conversion efficiency
Module evidence	12-couple tubular oxide generator: up to 20 mW at ΔT 389 °C	Demonstrates geometry and high-T operation	Phase impurity and contact resistance suppress output

7. Chhattisgarh-Specific Energy-Conversion Context

The purpose of a Chhattisgarh-specific analysis is not to assume a single state-wide waste-heat temperature; it is to map material families onto thermal opportunities that are plausible in an industrial region and then identify the measurements needed before deployment. The state's official investment portal describes large iron ore, coal and limestone reserves, major steel anchor units and surplus power with more than 26,000 MW installed capacity. These facts indicate a strong energy and metals-processing base. They do not provide heat-flux data, so the present paper treats steel/process surfaces, exhaust ducts, boilers and utility equipment only as candidate measurement locations for a future thermal survey. Climate affects the cold side. IMD climatological normals for Raipur (1991–2020) list an annual mean daily maximum of 33.0 °C and a May mean daily maximum of 41.8 °C. A passive air-cooled TEG can therefore face a significantly warmer T_c during summer than a laboratory test at 20–25 °C. From the efficiency equation, higher T_c reduces Carnot efficiency and can also move the thermoelectric legs away from their optimum mean temperature. This makes fin area, forced convection, water cooling where available, thermal spreaders and contact pressure first-order design variables. The same module may produce materially different power in May and in winter even if the hot source is unchanged.

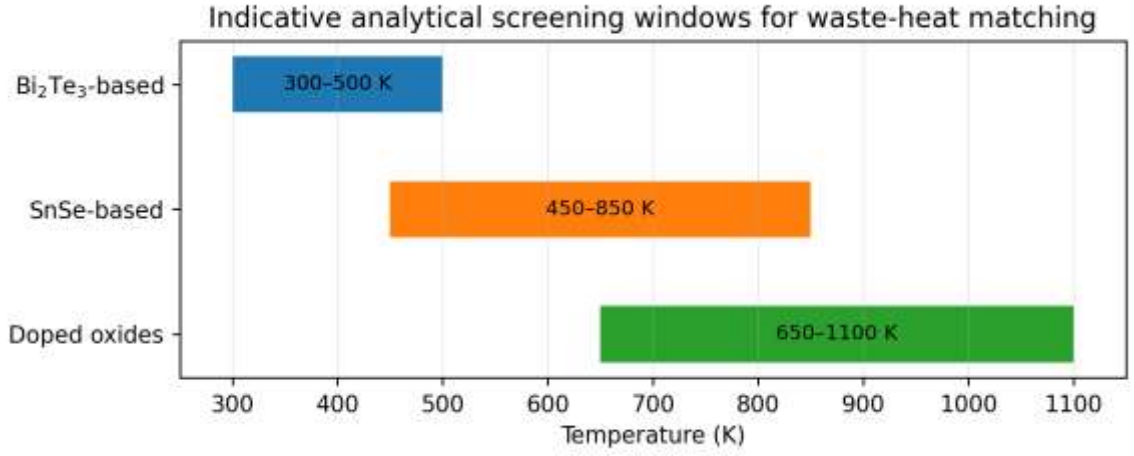

Figure 2. Indicative temperature windows used for analytical screening; these are design ranges, not hard material limits.

Table 6. Analytical mapping of candidate Chhattisgarh heat sources to thermoelectric material families.

Candidate thermal situation	Approx. screening hot-side range	Preferred material logic	Required pre-deployment measurement
Warm equipment / secondary process surfaces	350–500 K	Bi_2Te_3: strong near-room-temperature performance and mature modules	Surface temperature distribution, heat flux, duty cycle, available sink area

Medium-grade process exhaust / hot walls after primary recovery	500–750 K	SnSe: high average ZT potential across a broad gradient	Gas/surface temperature, oxidation exposure, vibration, thermal cycling
Hot oxidizing zone / high-temperature exhaust interface	700–1050 K	Doped oxides: stability-first option where chalcogenides need heavy protection	Maximum temperature, atmosphere, thermal shock, electrode compatibility
Cascaded or segmented source	Broad multistage range	Oxide → SnSe → Bi_2Te_3 can match progressively lower temperatures	Heat-exchanger pinch temperatures and inter-stage thermal resistance

A segmented approach is especially interesting because no single material is optimal from near ambient to 1000 K. A high-temperature oxide section can protect downstream stages from the harshest zone, SnSe can exploit the medium-temperature interval with high average ZT, and Bi_2Te_3 can harvest the final lower-grade gradient. The benefit is theoretical unless interfacial thermal resistance, electrical series resistance, differential thermal expansion and cost are controlled; consequently, segmentation should be a later-stage objective after single-material modules are characterized locally.

8. Analytical Performance Assessment Model

To compare the three material families on one thermodynamic basis, representative temperature scenarios are defined. These are not temperatures measured at a specific Chhattisgarh plant. They are screening cases chosen to reflect low-, medium- and high-grade heat with warm cold-side conditions. Effective average $Z\bar{T}$ values are intentionally more conservative than the highest published peak ZT for each family. This avoids the common analytical error of inserting a single peak ZT—often observed only over a narrow temperature interval—into a full-leg efficiency calculation.

Table 8. Input assumptions for the idealized performance screening.

Scenario	T_h (K)	T_c (K)	ΔT (K)	Effective $Z\bar{T}$	Reason for assumption
Bi_2Te_3 low-grade	423	313	110	1.15	Consistent with strong near-room-temperature bulk/film performance without using superlattice peak values
SnSe medium-grade	673	313	360	1.20	Conservative device-screening average; below best published SnSe $Z\bar{T}$ to account for realistic pair/module penalties
Doped oxide high-grade	873	323	550	0.25	Representative of improved $Ca_3Co_4O_9$-class performance while avoiding overstatement

$$\eta_{max} = (1 - T_c/T_h) \cdot [\ (\sqrt{(1+Z\bar{T})}-1) / (\sqrt{(1+Z\bar{T})}+T_c/T_h)\ ]$$

The model gives a material-level upper bound under constant-property and ideal-contact assumptions.

The model captures two distinct levers. First, temperature ratio sets the thermodynamic ceiling. Second, $Z\bar{T}$ determines the fraction of that ceiling that a thermoelectric material can approach. This means a high-temperature oxide can have a larger Carnot factor than Bi_2Te_3 but still show comparable or lower ideal efficiency if its ZT is much smaller. Conversely, SnSe can exploit both a larger ΔT and higher ZT, which is why it becomes the strongest performer in the medium-grade screening case.

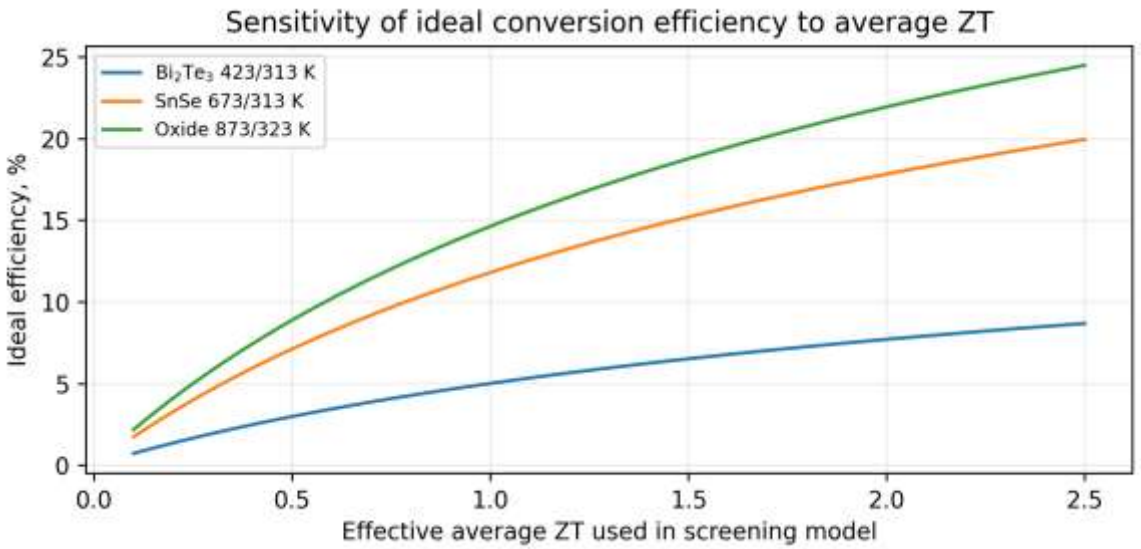

Figure 3. Sensitivity of ideal efficiency to average ZT for the three screening temperature pairs.

The sensitivity curves also show diminishing returns: at fixed temperature ratio, increasing ZT from very low values produces a large relative gain, but each additional unit of ZT yields a smaller incremental efficiency improvement. This supports parallel investment in thermal contacts, heat exchangers and electrical interfaces. Once intrinsic ZT is moderately high, a poorly coupled module can lose more power through parasitic resistance and heat leakage than is gained by a small laboratory increase in peak ZT.

9. Results and Comparative Performance

Table 9. Calculated ideal screening results.

Material case	T_h/Tc (K)	ΔT (K)	$Z\bar{T}$	Carnot η	Ideal TE η	Fraction of Carnot
Bi_2Te_3	423/313	110	1.15	26.0%	5.50%	21.1%
SnSe	673/313	360	1.20	53.5%	13.27%	24.8%
Doped oxide	873/323	550	0.25	63.0%	5.00%	7.9%

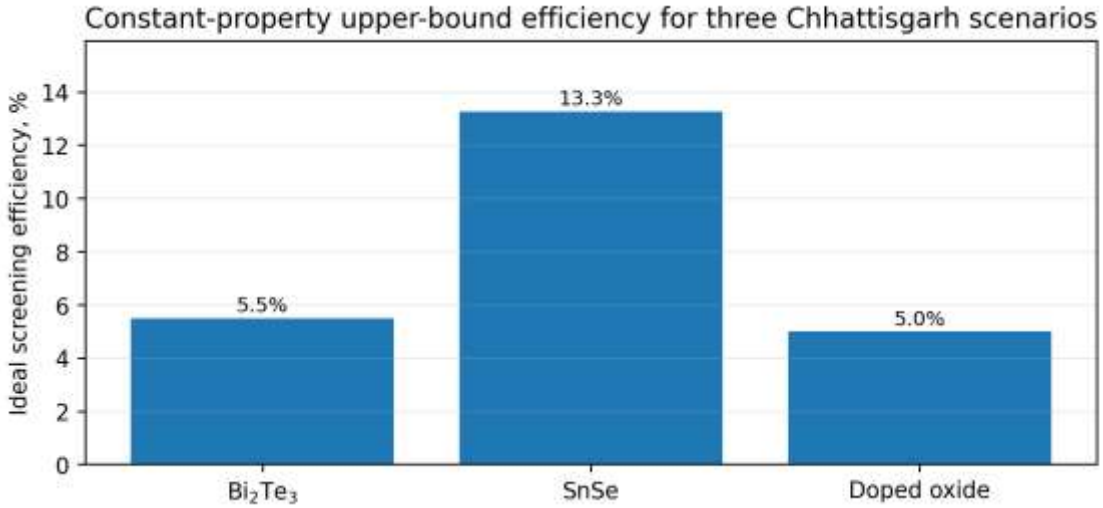

Figure 4. Idealized upper-bound conversion efficiency for the three analytical scenarios.

The SnSe case produces the highest ideal efficiency, approximately 13.3%, because it combines a substantial temperature ratio with a moderate-to-high assumed average ZT. The Bi_2Te_3 case gives about 5.5% at a much smaller ΔT of 110 K. This is not a poor result in context: low-grade heat has a low Carnot ceiling, so the proper question is whether the recovered electrical power justifies module area, heat exchanger and installation cost. The oxide case gives about 5.0% despite a 550 K temperature difference because the assumed $Z\bar{T}$ is only 0.25. The comparison demonstrates that temperature alone does not guarantee high thermoelectric efficiency.

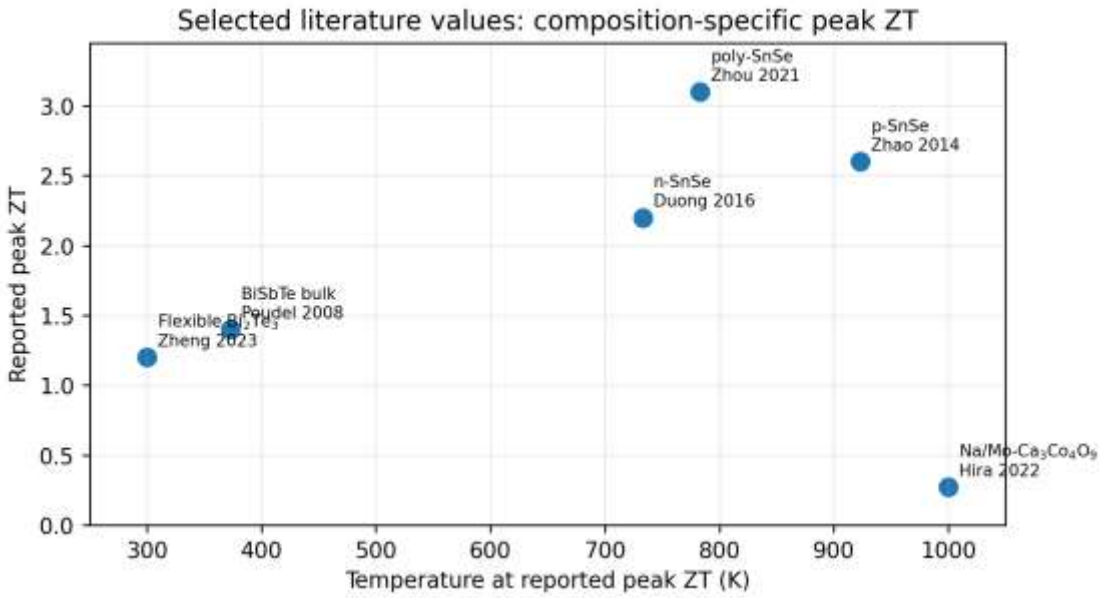

Figure 5. Selected reported peak ZT values from different studies and compositions; points are not a continuous material curve.

Figure 5 should not be read as a direct ranking of modules. The values were measured on different compositions, geometries, crystallographic directions and temperature intervals. In particular, a peak SnSe ZT above 3 does not imply that a practical SnSe module will operate at the corresponding ideal efficiency over its entire gradient. Similarly, oxide ZT appears modest, but oxide stability can permit use at temperatures where a high-ZT low-temperature material would be unsuitable. Device selection therefore requires both a transport metric and an operating-environment metric.

Measured device examples support this interpretation. Zheng et al. (2023) obtained 2.1 mW cm^{-2} from a flexible Bi_2Te_3 device at $\Delta T = 64$ K; Qin et al. (2023) measured approximately 8.9% single-leg efficiency in optimized p-type SnSe at $\Delta T \approx 300$ K; Merkulov et al. (2021) obtained up to 20 mW from a 12-couple oxide module at a 389 °C gradient. These outputs cannot be compared directly because device size, heat flow and contact architecture differ, but together they show that the material-to-device transition is already experimentally accessible for all three families.

10. Limitations of the Present Analysis

- The paper uses published material and device data obtained under different experimental protocols; cross-study values are therefore indicative, not perfectly normalized.
- The Chhattisgarh analysis does not include plant-specific heat-flux measurements, exhaust composition, operating hours, mechanical vibration or maintenance constraints.
- The ideal efficiency formula assumes a constant effective average ZT and does not solve coupled temperature-dependent transport with Thomson heat.
- No lifecycle assessment or levelized cost of recovered electricity is calculated because local material, module and installation cost data were not supplied.
- The reported device examples have different dimensions and heat flows, so power density and efficiency are discussed qualitatively rather than combined into one ranking.

11. Recommendations

- Begin with a thermal resource map at one representative Chhattisgarh industrial site. Measure surface/gas temperature, heat flux, duty cycle and available cold-side heat rejection for at least seasonal operating conditions.
- Use Bi_2Te_3 as the first low-grade baseline because mature commercial modules make it possible to separate heat-exchanger problems from materials-development problems.
- Develop purified, composition-controlled SnSe as the principal advanced-material research track for medium-grade waste heat. Measure anisotropic transport, texture, oxidation and contact resistance rather than ZT alone.
- Investigate Na/Mo- or rare-earth-modified $Ca_3Co_4O_9$ with a compatible n-type oxide for high-temperature durability trials. Prioritize phase purity, electrode compatibility and thermal cycling.
- Characterize temperature-dependent S(T), σ(T) and κ(T) and calculate device performance using segmented numerical integration before any scale-up; do not substitute peak ZT for average device behavior.

- Test electrical and thermal contact resistance before and after 100–500 thermal cycles. Contact degradation should be a go/no-go criterion for field deployment.
- For Raipur-area summer operation, design heat sinks for elevated ambient temperature and compare passive, forced-air and water-cooled configurations using net power after fan/pump consumption.
- After single-material modules are reliable, evaluate a segmented oxide–SnSe–Bi_2Te_3 architecture for broad-temperature sources. Segmentation should proceed only if added interfaces do not erase the theoretical efficiency gain.
- Assess lifetime energy yield, material availability, repairability and end-of-life handling together with electrical efficiency so that "sustainable" refers to the full deployment rather than only heat recovery.

12. Conclusion

Advanced thermoelectric materials offer a physically credible route for distributed waste-heat recovery in Chhattisgarh, but their usefulness depends on matching transport physics to temperature, atmosphere and module engineering. Bi_2Te_3-based materials remain the strongest near-room-temperature option and benefit from the most mature module technology. SnSe offers the largest performance headroom, supported by exceptionally high peak ZT, improved polycrystalline processing, high average ZT and measured single-leg efficiencies near 9% in optimized crystals. Doped oxides provide lower conversion efficiency but extend the design space toward hotter oxidizing environments where chemical robustness can be more important than record ZT. The common analytical model reinforces this hierarchy. Under representative, deliberately conservative screening assumptions, ideal efficiencies are about 5.5% for low-grade Bi_2Te_3, 13.3% for medium-grade SnSe and 5.0% for a high-grade doped oxide case. These are upper bounds, not field predictions. Their purpose is to show the coupled influence of temperature ratio and average ZT and to prevent overinterpretation of peak ZT values. The analysis further shows that Chhattisgarh's warm summer ambient can materially reduce low-grade performance unless the cold side is engineered carefully.

The most important conclusion is methodological: a successful Chhattisgarh thermoelectric program should move from thermal mapping to material screening, from material screening to contact-qualified modules, and from modules to long-duration field pilots. The technology should be applied where distributed heat, low maintenance and solid-state operation create system value. With that sequence, thermoelectric development can complement conventional recovery methods and convert otherwise rejected heat into useful electricity while generating locally relevant experimental knowledge in solid-state and energy-conversion physics.

References

Choi, S.-M., Lee, K.-H., Lim, C.-H., & Seo, W.-S. (2011). Oxide-based thermoelectric power generation module using p-type $Ca_3Co_4O_9$ and n-type $(ZnO)_7In_2O_3$ legs. Energy Conversion and Management, 52(1), 335–339. https://doi.org/10.1016/j.enconman.2010.07.005

Duong, A. T., Nguyen, V. Q., Duvjir, G., Duong, V. T., Kwon, S., Song, J. Y., Lee, J. K., Lee, J. E., Park, S., Min, T., Lee, J., & Kim, J. (2016). Achieving ZT = 2.2 with Bi-doped n-type SnSe single crystals. Nature Communications, 7, 13713. https://doi.org/10.1038/ncomms13713

Government of Chhattisgarh, Department of Commerce & Industries. (2026). Steel: Growth drivers and competitive advantages. Chhattisgarh Business Made Easy. Accessed 9 August 2026.

Hira, U., Ali, S. S., Latif, S., Pryds, N., & Sher, F. (2022). Improved high-temperature thermoelectric properties of dual-doped $Ca_3Co_4O_9$. ACS Omega, 7(8), 6579–6590. https://doi.org/10.1021/acsomega.1c05721

India Meteorological Department. (n.d.). Climatological table, station 42874 (Raipur), period 1991–2020. Accessed 9 August 2026.

Merkulov, O. V., Lopes, D., Markov, A. A., Ferreira, N. M., Patrakeev, M. V., & Kovalevsky, A. V. (2021). Tubular thermoelectric module based on oxide elements grown by the laser floating zone. ACS Applied Energy Materials, 4(6), 5848–5857. https://doi.org/10.1021/acsaem.1c00677

Poudel, B., Hao, Q., Ma, Y., Lan, Y., Minnich, A., Yu, B., Yan, X., Wang, D., Muto, A., Vashaee, D., Chen, X., Liu, J., Dresselhaus, M. S., Chen, G., & Ren, Z. (2008). High-thermoelectric performance of nanostructured bismuth antimony telluride bulk alloys. Science, 320(5876), 634–638. https://doi.org/10.1126/science.1156446

Qin, B., Wang, D., Hong, T., Wang, Y., Liu, D., Wang, Z., Gao, X., Ge, Z.-H., & Zhao, L.-D. (2023). High thermoelectric efficiency realized in SnSe crystals via structural modulation. Nature Communications, 14, 1366. https://doi.org/10.1038/s41467-023-37114-7

Saini, S., Yaddanapudi, H. S., Tian, K., Yin, Y., Magginetti, D., & Tiwari, A. (2017). Terbium ion doping in $Ca_3Co_4O_9$: A step towards high-performance thermoelectric materials. Scientific Reports, 7, 44621. https://doi.org/10.1038/srep44621

Shi, H., Wen, Y., Bai, S., et al. (2025). Crystal symmetry modification enables high-ranged in-plane thermoelectric performance in n-type SnSe crystals. Nature Communications, 16, 1788. https://doi.org/10.1038/s41467-025-57125-w

Venkatasubramanian, R., Siivola, E., Colpitts, T., & O'Quinn, B. (2001). Thin-film thermoelectric devices with high room-temperature figures of merit. Nature, 413, 597–602. https://doi.org/10.1038/35098012